第33卷第4期
2014年8月

红外与毫米波学报
J. Infrared Millim. Waves

Vol. 33, No. 4
August, 2014

文章编号:1001-9014(2014)04-0349-06

DOI:10.3724/SP.J.1010.2014.00349

Transverse spin currents through a three-arm ring embedded with two quantum dots

LIANG Feng[1*], GU Yu[2]

(1. Department of Physics, Huaiyin Institute of Technology, Huai'an 223003, China
2. Department of Physics and Siyuan Laboratory, Jinan University, Guangzhou 510632, China)

Abstract: The spin-polarized electron transport through a three-terminal three-arm ring with two quantum dots separately embedded in the upper and lower arms were theoretically studied. The intradot Coulomb interaction on the two dots and the Rashba spin-orbit interaction inside one arm of the ring were taken into account. With the aid of the nonequilibrium Green's function method, we find that even without using any magnetic factors a Rashba induced spin interference effect can drive a spin-polarized current out of the device. By properly tuning the system parameters such as the applied external voltages, the Rashba interaction strength and the dot levels, not only a fully spin-polarized current but also a pure spin current can be obtained. Moreover, the effects of the system parameters on the magnitude, sign, spin-polarization and resonant peaks of the spin-polarized current were also discussed.

Key words: quantum ring, quantum dot, spin current, nonequilibrium Green's function
PACS: 72.25. Dc, 73.23.-b, 73.63.-b

嵌有两个量子点的三终端量子环中的横向自旋流

梁 峰[1*], 古 宇[2]

(1. 淮阴工学院 数理学院,江苏 淮安 223003; 2. 暨南大学 物理系与思源实验室,广东 广州 510632)

摘要:从理论上研究了一个上臂与下臂各嵌有一个量子点的三终端三臂量子环中的自旋极化的电子输运性质.考虑了两个量子点中的库仑互作用并假设在某一个环臂中存在Rashba自旋轨道耦合作用.利用非平衡态格林函数方法,发现不需要借助任何磁场与磁性物质Rashba自旋轨道耦合作用导致的量子干涉效应就可以从器件中驱动出一个自旋流.适当调节外加偏压、Rashba自旋轨道耦合作用强度以及量子点能级等系统参数时器件中甚至还可以产生完全自旋极化电流或纯自旋流.另外,还讨论了系统参数对自旋流大小、符号、自旋极化度以及峰值的影响.

关 键 词:量子点环;量子点;自旋流;非平衡格林函数

中图分类号:O488 **文献标识码**:A

Introduction

In recent years, spintronics has been one of the most interesting areas of condensed matter physics, which aims to exploit the charge and spin degrees of freedom of electrons in spin devices. One of the current challenges in spintronics is how to effectively generate and manipulate a spin-polarized current in various mesoscopic systems. Till now, much methods from both experimental and theoretical physics communities have been put forward to overcoming the challenge. The traditional methods to generate a spin-polarized current are mainly optical and magnetic ones including optical spin orientation methods[1-2], spin injection across a magnetic-nonmagnetic interface[3-4] and adiabatic or non-adiabatic spin pumping[5-7] with the usage of time-varying magnetic fields. However, all the above-mentioned methods have serious drawbacks in practice. For example, optical methods are difficult to be integrated into an electric circuit, the efficiency of spin injection from ferromagnetic metal into a semiconductor is still unsatisfactory due to the conductiv-

Received date: 2013-04-24, **revised date**: 2014-05-23 **收稿日期**:2013-04-24, **修回日期**:2014-05-23
Foundation items: Supported by NSFC (11147147), Distinguished Young Talents in Higer Education of Guangdong China (LYM11021), Research Training and Innovation Fund of Jinan University (21612439) and Young Teacher Fund of Huaiyin Institute of Technology (2717577).
Biography: LIANG Feng(1982-), male, Jiangsu Huaian, Doctor, Research fields focus on quantum transport in nanostructures.
* **Corresponding author**: E-mail: bd10583@163.com

ity mismatch and for spin pumping methods magnetic fields may destroy the spin coherence of electrons. Therefore, it is more desirable to generate and control a spin-polarized current in nanostructures by an all-electrical method.

Since Datta and Das proposed the spin field effect transistor more than two decades ago[8], Rashba spin-orbit interaction (RSOI) has greatly attracted research attention. The RSOI, which is a relativistic effect at a low speed limit, couples the spin degree of freedom of electron to its orbit motion and it's strength can be conveniently controlled by an external electric field or a gate voltage[9], thus offering a promising all-electrical approach to manipulate the electron spin. In fact, there have already been some works concerning about electrically realizing spin-dependent transport via quantum spin interference effect in various kinds of multi-path devices[10-13]. Most of these works are based on the RSOI induced Aharonov-Casher (AC) phase which results from the electron spin precessing about the effective magnetic field induced by the RSOI when the electron moves through a regime in the presence of RSOI. Different from the well-known Aharonov-Bohm (AB) phase, which is a spin-independent geometric phase induced by a magnetic flux, the AC phase is a spin-dependent one and can cause a spin interference effect in a multi-path device, since such a device can provide more than one Feynman path for the propagation of electron waves. The spin interference effect makes the phase coherent transport process in the mesoscopic device spin-resolved and thus leads to a spin-polarized current or a spin accumulation in the system. However, due to the phase locking effect [13-14], the outflowing current can never be spin-polarized in a two-terminal spin interference effect device. Therefore, in order to obtain an outflowing spin-polarized current purely by the spin interference effect, a three-terminal or multi-terminal device is always required.

In the present paper, we investigate the spin-dependent transport through a three-arm ring with two embedded quantum dots (QDs) where intradot Coulomb interaction and RSOI are both taken into account. To avoid the phase locking effect, the two-dot three-arm ring is connected to three normal leads. Then due to the coexistence of different Feynman paths and a local RSOI, when an electron wave propagates from one lead to another one, a spin interference effect can occur and result in a spin-polarized current flowing in the leads. By the Keldysh nonequilibrium Green's function method, we have analyzed the resulting spin-polarized current in the investigated system. Our results show that the magnitude, spin-polarization and current peaks of the generated spin-polarized current can be conveniently controlled by the system parameters such as the applied external voltages, the strength of the RSOI, the dot levels and the lead-lead coupling strength. Of particular interest, even only one spin component current can survive and another spin component one is fully suppressed by appropriately adjusting the system parameters, i. e., a fully spin-polarized current can be achieved, in other words, the spin injection with 100% can be realized in our proposed device. Furthermore, at a certain constellation of the system parameters, an equal spin-up and spin-down charge currents can flow oppositely through the device, i. e., a pure spin current without any accompanying charge current can also be obtained, which has been one of the focuses of spintronics research.

The rest of this paper is organized as follows. In Sec. 2, we present the second-quantized model Hamiltonian for the proposed device and derive the formula of the spin-polarized current by using the nonequilibrium Green's function method. In Sec. 3, we study the properties of the spin-polarized current numerically. Finally, a brief conclusion is given in Sec. 4.

1 Physical model and formula

The device of interest is depicted in Fig. 1, which is composed of three normal metal leads and a three-arm ring with two quantum dots (QDs) sitting on the upper and lower arms respectively. Owing to the small effective mass, the energy separation between single electron levels in semiconductors is considerably sizable. Hence, only a single energy level near the Fermi face is assumed to be involved in each QD. For the studied system, we assume that there exists a local RSOI in the arm between QD2 and the right lead. The intradot Coulomb interaction is also considered for each QD and for simplicity we assume that the intradot Coulomb interactions in the two QDs have the same strength. The left and right leads are connected to each dot, while the middle lead is only connected to QD1. In addition, the left and right leads are also directly coupled together through the middle arm of the ring. Due to the device configuration, when an electron wave propagates from one lead to another one, more than one Feynman path can be followed and the electron wave following the path through QD2 can acquire an AC phase due to the RSOI induced spin precession. Consequently, a spin-resolved interference effect between different paths can take place, and thus a spin-polarized current may emerge in the system. For the considered device, the total Hamiltonian in second-quantized form can be written as

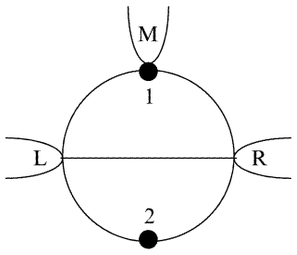

Fig. 1 Schematic of a three-terminal spin device, which consists of tree normal metal leads and a three-arm ring embedded with two QDs
图1 由三个普通金属电极与一个嵌有两个量子点的三臂量子环构成的三终端自旋电子器件

$$H = H_0 + H_D + H_T \quad , \quad (1)$$

$$H_0 = \sum_{k\alpha\sigma} \varepsilon_{k\alpha} C^+_{k\alpha\sigma} C_{k\alpha\sigma} + \left(\sum_{i\sigma} \varepsilon_i d^+_{i\sigma} d_{i\sigma} + U n_{i\uparrow} n_{i\downarrow} \right) \quad , (2)$$

$$H_D = \sum_{kk'\sigma} t_{LR} \left(C^+_{kL\sigma} C_{k'R\sigma} + C^+_{k'R\sigma} C_{kL\sigma} \right) \quad , \quad (3)$$

$$H_T = \sum_{ik\sigma} t_{Li} C^+_{kL\sigma} d_{i\sigma} + t_{R1} C^+_{kR\sigma} d_{1\sigma} + t_{R2} e^{-i\sigma\varphi} C^+_{kR\sigma} d_{2\sigma} + t_{M1} C^+_{kM\sigma} d_{1\sigma} + h.c. \quad , (4)$$

where the operator $d_{i\sigma}^{+}$ ($d_{i\sigma}$) creates (destroys) an electron with spin σ ($\sigma = \uparrow, \downarrow or \sigma = \pm$) in QDi ($i = 1,2$), $C_{k\alpha\sigma}^{+}$ ($C_{k\alpha\sigma}$) creates (destroys) a conduction electron with spin σ and wavevetor k in lead α ($\alpha = L,R,M$), and $n_{i\sigma} = d_{i\sigma}^{+} d_{i\sigma}$ is the number operator for the corresponding state of the dot spin. The first term in H_0 describes the three leads, which are described by the noninteracting free electron gas model. The second and third terms in H_0 correspond to the isolated QDs, each of which has one energy level ε_i and an intradot Coulomb interaction with the interaction strength U. The term H_D accounts for the direct coupling between the left and right leads via the middle arm with the coupling strength t_{LR}. The last term H_T describes the couplings of the dots to the leads, where $t_{\alpha i}$ is the hopping matrix element between lead α and QDi. Since the local RSOI is considered, a spin-dependent AC phase $\sigma\varphi = \sigma\alpha_R mL/\hbar^2$ enters into the hopping matrix element modeling electron's tunneling between QD2 and the right lead, with α_R being the RSOI strength parameter, m being the effective mass of electrons and L being the length of the arm between QD2 and the right lead.

Our focus is the tunneling current from the middle lead to QD1. According to the Heisenberg equation of motion, the charge current per spin channel flowing from the middle lead to the dot can be calculated from the time evolution of the occupation number of electrons with the corresponding spin in the middle lead, i. e. , the spin component current can be evaluated by

$$I_\sigma = -e < dN_{M\sigma}/dt > = \frac{ie}{\hbar} < [N_{M\sigma}, H] >,$$
$$N_{M\sigma} = \sum_k C_{kM\sigma}^{+} C_{kM\sigma} \quad , \quad (5)$$

with $[\ldots]$ and $<\ldots>$ denoting operator commutation and the quantum statistical average respectively. Then with use of the Keldysh Green's function method[15] the spin component current flowing in the middle lead can be expressed as

$$I_\sigma = \frac{e}{\hbar}\int \frac{d\omega}{2\pi} [t_{M1} G_{1M\sigma}^{<}(\omega) + h.c.] \quad , \quad (6)$$

where $G_\sigma^{<}(\omega)$ is the Fourier transform of the lesser Green's fuction $G_\sigma^{<}(t)$. In the local basis $G_\sigma^{<}(t)$ is a 5×5 matrix, whose matrix elements are

$$G_{\alpha\alpha'\sigma}^{<}(t) = i < \sum_{k'} C_{k'\alpha'\sigma}^{+}(0) \sum_k C_{k\alpha\sigma}(t) > \quad (\alpha,\alpha' = L,R,M) \quad , \quad (7)$$
$$G_{\alpha i\sigma}^{<}(t) = i < d_{i\sigma}^{+}(0) \sum_k C_{k\alpha\sigma}(t) > \quad (\alpha = L,R,M; i = 1,2) \quad , \quad (8)$$
$$G_{i\alpha\sigma}^{<}(t) = i < \sum_k C_{k\alpha\sigma}^{+}(0) d_{i\sigma}(t) > \quad (\alpha = L,R,M; i = 1,2) \quad , \quad (9)$$
$$G_{ij\sigma}^{<}(t) = i < d_{j\sigma}^{+}(0) d_{i\sigma}(t) > \quad (i,j = 1,2) \quad . \quad (10)$$

The above lesser Green's functions are related to the retarded and advanced Green's functions through the well-known Keldysh equation,

$$G_\sigma^{<} = G_\sigma^{r} g_\sigma^{r-1} g_\sigma^{<} g_\sigma^{a-1} G_\sigma^{a} + G_\sigma^{r} \Sigma_\sigma^{<} G_\sigma^{a} \quad , \quad (11)$$

here G_σ^{r} is the retarded Green's function of the system and G_σ^{a} is the advanced Green's function whose expression is the Hermitian conjugate of G_σ^{r}. In the local basis G_σ^{r} is also a 5×5 matrix with matrix elements defined as

$$G_{\alpha\alpha'\sigma}^{r}(t) = -i\theta(t) < [\sum_k C_{k\alpha\sigma}(t), \sum_{k'} C_{k'\alpha'\sigma}^{+}(0)]_+ > \quad (\alpha,\alpha' = L,R,M) \quad , \quad (12)$$
$$G_{i\alpha\sigma}^{r}(t) = -i\theta(t) < [d_{i\sigma}(t), \sum_k C_{k\alpha\sigma}^{+}(0)]_+ > \quad (\alpha = L,R,M; i = 1,2) \quad , \quad (13)$$
$$G_{\alpha i\sigma}^{r}(t) = -i\theta(t) < [\sum_k C_{k\alpha\sigma}(t), d_{i\sigma}^{+}(0)]_+ > \quad (\alpha = L,R,M; i = 1,2) \quad , \quad (14)$$
$$G_{ij\sigma}^{r}(t) = -i\theta(t) < [d_{i\sigma}(t), d_{j\sigma}^{+}(0)]_+ > \quad (i,j = 1,2) \quad , \quad (15)$$

where $[\ldots]_+$ denotes the anticommutation relation. In Eq. (11) $g_\sigma^{r(a,<)}$ stand for the corresponding Green's functions for the uncoupled system (i. e, $t_{LR} = t_{\alpha i} = 0$) and $\Sigma_\sigma^{<}$ stands for the lesser self energy. For our system, $\Sigma_\sigma^{<} = 0$ and $g_\sigma^{r-1} g_\sigma^{<} g_\sigma^{a-1}$ is diagonal

$$g_\sigma^{r-1} g_\sigma^{<} g_\sigma^{a-1} = \begin{bmatrix} 2if_L(\omega)/\pi\rho & 0 & 0 & 0 & 0 \\ 0 & 2if_R(\omega)/\pi\rho & 0 & 0 & 0 \\ 0 & 0 & 2if_M(\omega)/\pi\rho & 0 & 0 \\ 0 & 0 & 0 & 0 & 0 \\ 0 & 0 & 0 & 0 & 0 \end{bmatrix}, \quad (16)$$

where $f_\alpha(\omega) = 1/[e^{(\omega-\mu_\alpha)/k_B T} + 1]$ is the Fermi distribution function of lead α and ρ is the density of states of leads. In order to solve the retarded Green's function G_σ^{r}, we adopt the Dyson equation

$$G_\sigma^{r} = (g_\sigma^{r-1} - \Sigma_\sigma^{r})^{-1} \quad . \quad (17)$$

In the wide-band approximation[15] the retarded Green's function of the uncoupled system g_σ^{r} can be expressed in the form

$$g_\sigma^{r} = \begin{bmatrix} -i\pi\rho & 0 & 0 & 0 & 0 \\ 0 & -i\pi\rho & 0 & 0 & 0 \\ 0 & 0 & -i\pi\rho & 0 & 0 \\ 0 & 0 & 0 & g_{11\sigma}^{r} & 0 \\ 0 & 0 & 0 & 0 & g_{22\sigma}^{r} \end{bmatrix}, \quad (18)$$

with $g_{ii\sigma}^{r}$ being the retarded Green's functions of the isolated ith QD which can be written as $g_{ii\sigma}^{r} = \frac{\omega - \varepsilon_i - U + Un_{i-\sigma}}{(\omega-\varepsilon_i)(\omega-\varepsilon_i-U)}$ in the Hartree-Fock approximation. In addition, the self-energy neglecting higer-order terms can be given by the tunneling matrix

$$\Sigma_\sigma^{r} = \begin{bmatrix} 0 & t_{LR} & 0 & t_{L1} & t_{L2} \\ t_{LR} & 0 & 0 & t_{R1} & t_{R2} e^{-i\sigma\varphi} \\ 0 & 0 & 0 & t_{M1} & 0 \\ t_{L1} & t_{R1} & t_{M1} & 0 & 0 \\ t_{L2} & t_{R2} e^{i\sigma\varphi} & 0 & 0 & 0 \end{bmatrix}. \quad (19)$$

As the final step, the occupation number in $g_{ii\sigma}^{r}$ is determined by the following equation

$$n_{i\sigma} = -i\int \frac{d\omega}{2\pi} G_{ii\sigma}^{<}(\omega) \quad , \quad (20)$$

with $G_{ii\sigma}^{<}(\omega) = \frac{2i}{\pi\rho}\sum_\alpha |G_{i\alpha\sigma}^{r}(\omega)|^2 f_\alpha(\omega)$. With the above equations, the spin component current I_σ can be solved self-consistently and then the charge and spin current in the middle lead can also be worked out as follows

$$I_M = I_\uparrow + I_\downarrow, J_M = I_\uparrow - I_\downarrow \quad . \quad (21)$$

2 Results and discussions

In this section, we present numerical results to show some interesting properties of the generated spin-polarized current in the studied system. During the numerical evaluation we assume that the energy 100 meV to be the unit of energy and 0.01 meV^{-1} to be the unit of density of state. Because the wide-band approximation is adopted in the evaluation of the self energies, the density of states in leads have been assumed to be independent of energies, and in our calculations we set $\rho_L = \rho_R = \rho_M = 1$. The Fermi energy of each lead is taken as the origin of energy, so that the electrochemical potential of lead α is $\mu_\alpha = V_\alpha$ with V_α being the external voltage applied on the corresponding lead. Fig. 2 shows the two spin component currents as a function of the voltage V_R with the other parameters fixed. It is clear that the spin-up and spin-down currents can be modulated by the voltage V_R in both magnitude and flowing direction and when V_R varies in the given region the difference between the two spin component currents is nonzero, i. e., a spin-polarized current is generated. At point A ($V_R \approx -0.6$in Fig. 2(a) or $V_R \approx -2.01$in Fig. 2(b)), the spin-down current vanishes while the spin-up one survives, hence a fully spin-polarized current with up-spin emerges in the middle lead. On the contrary, at point B($V_R \approx -0.32$ in Fig. 2(a) or $V_R \approx -1.26$ in Fig. 2(b)), the suppressed current is the spin-up one and another type of fully spin-polarized current with down-spin emerges, of which the following direction is opposite to that of the spin-up one obtained at point A. More interestingly, when $V_R \approx -0.5$ for $U = 1.0$ or $V_R \approx -0.1$ for $U = 0.0$(see point C in Fig. 2(a) and Fig. 2(b)), the spin-up and spin-down currents flow in opposite directions and have identical magnitudes, thus a pure spin current without any accompanying charge one forms in the middle lead.

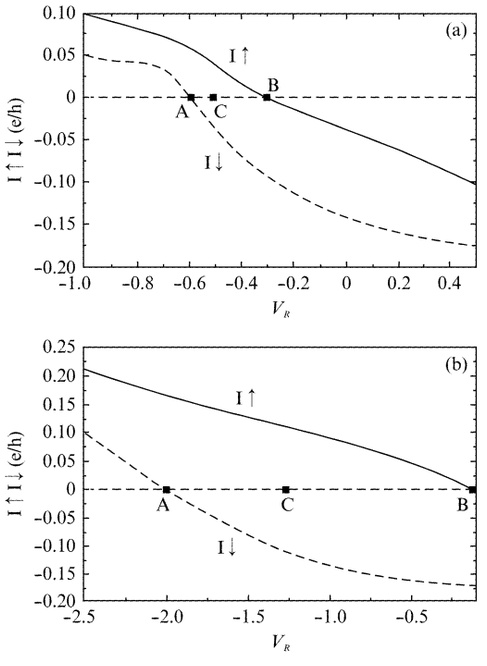

Fig. 2 The induced two spin component currents versus the external voltage V_R with $t_{L1} = t_{R1} = t_{LR} = 0.4$, $t_{L2} = t_{R2} = t_{M1} = 0.8$, $V_L = 1.0$, $V_M = 0.0$, $\varepsilon_1 = 1.0$, $\varepsilon_2 = -0.1$, $k_BT = 0.02$, $\varphi = \pi/3$ for. (a) $U = 1.0$, and (b) $U = 0$

图2 两个自旋分流与外加偏压 V_R 的关系. 其中 $t_{L1} = t_{R1} = t_{LR} = 0.4$, $t_{L2} = t_{R2} = t_{M1} = 0.8$, $V_L = 1.0$, $V_M = 0.0$, $\varepsilon_1 = 1.0$, $\varepsilon_2 = -0.1$, $k_BT = 0.02$, $\varphi = \pi/3$. (a) $U = 1.0$, (b) $U = 0$

Next we present the dependence of the two spin component currents on the AC phase φ, which can be tuned by adjusting the RSOI strength with an electric field or a gate voltage. As depicted in Fig. 3, both the spin-up and spin-down current oscillates with φ and exhibits a sinusoidal-like behavior when the other parameters are fixed. In general, the two spin component currents are out of phase thus giving rise to a spin-polarized current. The destruction of the origin symmetry of the two spin component currents arises from the spin-dependent interference effect induced by the AC phase due to the local RSOI. Hence, at point $A_1(\varphi = 0)$, the RSOI is absent and the outflowing current in the middle lead is unpolarized. However, at point$A_2(\varphi = \pi)$ and point $A_3(\varphi = 2\pi)$, the current is also unpolarized, this is because the RSOI induced spin interference effect reaches it's fully destructive points at$\varphi = n\pi$ ($n = \pm 1, \pm 2, \pm 3\ldots$). Of particular interest, at pointsB_1, B_2, B_3 and B_4, only one spin component current survives and another one vanishes totally so that a fully spin-polarized current can be obtained. Moreover, at pointC_1 ($\varphi = 0.37$) and pointC_2 ($\varphi = 1.64$), the two spin component currents are equal in magnitude but have opposite following directions, thus a pure spin current can also be obtained. By present experimental technology, the phase φ is tunable to a large extent. For example, if the RSOC strength parameter$\alpha_R = 3 \times 10^{-11}$eVm, the effective mass $m = 0.036m_e$[16], and the length of the arm between QD2 and the right lead is 200 nm, then $\sigma\varphi = \sigma\alpha_R mL/\hbar^2 \approx \pi$. Therefore, in experiments the generation of a fully spin-polarized current or a pure spin current by electrically tuning the AC phase can be realized.

In the following, we proceed to investigate the

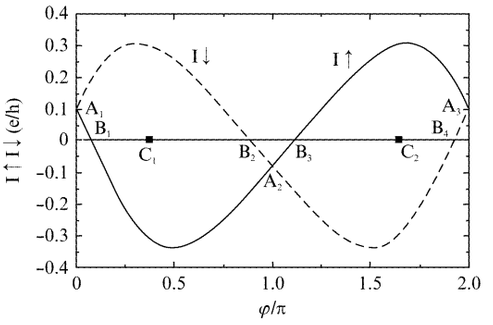

Fig. 3 The induced two spin component currents versus φ with $t_{LR} = 0.1$, $t_{L2} = t_{R2} = 0.4$, $V_R = -1.0$, $\varepsilon_2 = 1.0$, $U = 2.0$ and the other parameters chosen as in Fig. 2

图3 两个自旋分流与 φ 的关系. 其中 $t_{LR} = 0.1$, $t_{L2} = t_{R2} = 0.4$, $V_R = -1.0$, $\varepsilon_2 = 1.0$, $U = 2.0$, 其他参数的选取与图2相同

charge and spin current in the middle lead when one of the QD levels is fixed. In Fig. 4(a), we show the dependence of I_M and J_M on the QD level ε_2 with fixed $\varepsilon_1 = 0$ for U = 0 and in Fig. 4(b) we show the same dependence for U = 2. It is shown that not only the magnitude but also the sign of the generated spin current can be strongly modulated by ε_2, which can be easily controlled by a gate voltage. When U = 0, as Fig. 4(a) shows, both the charge and spin current has two antisymmetric resonant peaks, which can be attributed to the fano resonance. The fano resonance here arises from the quantum interference between the discrete channels and the continuum channel since the electron wave can propagate through both the QDs (discrete channels) and the direct channel between the left and right leads (continuum channel). Because the generated spin current originates from the charge current with the spin interference effect, it also exhibits an antisymmetric behavior. This antisymmetry of the spin current allows us to change the sign of the spin current easily. In Fig. 4(b), every resonant peak in Fig. 4(a) evolves to two peaks, the two emerging peaks are obviously the result from the Coulomb blockade effect induced by the nonzero intradot Coulomb interaction. Fig. 4 also indicates that the spin-polarization of the spin-polarized current which is defined as $\eta = J_M/I_M$ can also be modulated in a large range, since the charge and spin current changes out of phase with the adjustment of ε_2. Especially, at those points where $I_M = J_M$ the spin-polarization is equal to 100% and at those points where $I_M = 0, J_M \neq 0$ the spin-polarization is equal to infinity indicating that both a fully spin-polarized current and a pure spin current can be generated only if the value of ε_2 is chosen properly. In addition, with the increase of the magnitude of ε_2, the spin current tends to be zero, the reason for this effect is that a too large magnitude of ε_2 can strongly weaken the possibility of electrons´ tunneling through QD2, so that the transport of electrons in the arm embedded with QD2 is almost forbidden and then the spin interference effect which is a prerequisite for the generation of the spin current is destroyed.

Then we focus on the properties of the spin-polarized current in the middle lead as it is not a pure spin current. In Fig. 5, the spin current and the spin-polarization versus the coupling strength t_{LR} are plotted for different φ. As can be seen, the magnitude of the spin current and the spin-polarization can be modulated by t_{LR}. With the increase of t_{LR}, the value of spin current and the spin-polarization increases firstly and then decreases gradually to be zero after it reaches a peak value. The underlying physics responsible for the disappearance of the spin current or spin-polarization at a large t_{LR} is that a large t_{LR} makes electron waves prefer to propagate through the middle arm and the propagation of electron waves through the arm embedded with QD2 is almost prevented, so that the spin interference effect is greatly weaken, thus resulting in the suppression of the spin current. Moreover, Fig. 5(b) shows that the magnitude of the spin-polarization is tunable in a large range by adjusting t_{LR} and under some circumstances a fully spin-polarized current can be obtained, which is sizable as shown in Fig. 5(a). Finally, we would like to point out that all the system parameters such as the AC phase, the dot levels and the lead-lead coupling strength can be conveniently adjusted by an electric field or a gate voltage without using any magnetic

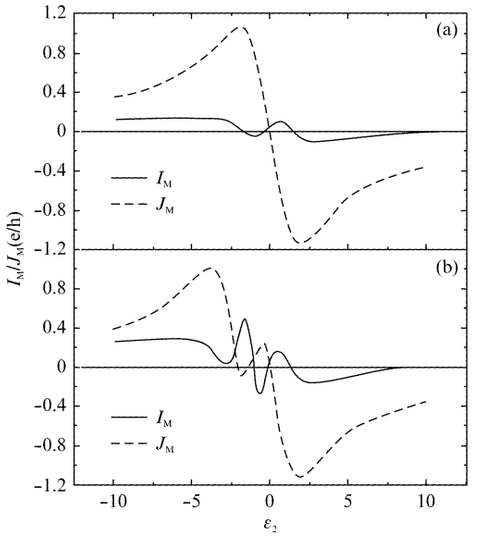

Fig. 4　The charge and spin current versus ε_2 with $\varepsilon_1 = 0$ for (a) $U = 0$, and (b) $U = 2.0$. The other parameters are $t_{L1} = t_{R1} = t_{L2} = t_{R2} = 0.8$, $t_{LR} = 0.1$, $t_{M1} = 0.8$, $V_L = 1.0$, $V_M = 0.0$, $V_R = -1.0$, $k_BT = 0.02$ and $\varphi = 0.6$

图 4　电流以及自旋流与 ε_2 的关系. (a) $U = 0$, (b) $U = 2.0$. 其他参数为 $t_{L1} = t_{R1} = t_{L2} = t_{R2} = 0.8$, $t_{LR} = 0.1$, $t_{M1} = 0.8$, $V_L = 1.0$, $V_M = 0.0$, $V_R = -1.0$, $k_BT = 0.02$, $\varphi = 0.6$

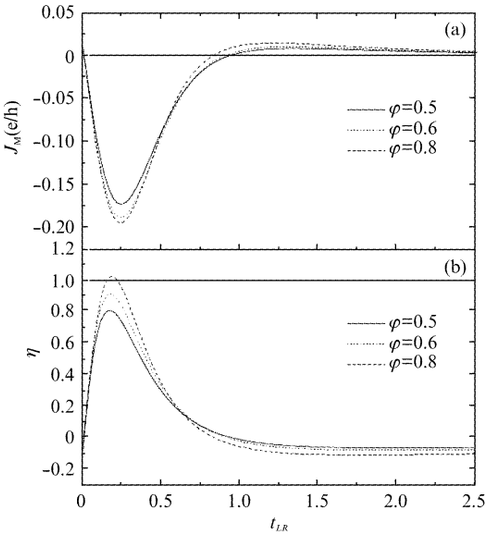

Fig. 5　(a) The generated spin current and (b) the spin-polarization of the generated spin-polarized current versus the coupling strength t_{LR} with $\varepsilon_1 = 1.0$, $\varepsilon_2 = -1.0$, $t_{L1} = t_{R1} = t_{L2} = t_{R2} = 0.4$ for different phase φ. The other parameters are chosen as in Fig. 4(b)

图 5　(a) 自旋流和(b) 自旋流的自旋极化度在选取不同的 φ 时与耦合强度 t_{LR} 的关系, 其中 $\varepsilon_1 = 1.0$, $\varepsilon_2 = -1.0$, $t_{L1} = t_{R1} = t_{L2} = t_{R2} = 0.4$. 其他参数的选取与 Fig. 4(b) 相同

factors. Therefore, the generation and manipulation of the spin current in our proposed device are all-electrical.

3 Conclusions

In conclusion, a new device composed of a two-dot three-arm ring and three normal leads was proposed. Based on the Keldysh nonequilibrium Green's function method, the spin-polarized transport through the device has been investigated considering both the Coulomb interaction and RSOI. The results show that the AC phase induced spin interference effect can give rise to a transverse spin-polarized current in the middle lead. By tuning the system parameters, the magnitude, sign, resonant peaks and even the spin-polarization of the generated current can be easily modulated. In particular, a proper adjustment of these parameters can produce a fully spin-polarized current or a pure spin current. Since all the parameters can be tuned electrically, our proposal may act as a promising all-electrical spin device for the generation and manipulation of the spin current.

References

[1] Hubner J, Ruhle W W, Klude M, *et al*. Direct observation of optically injected spin-polarized currents in semiconductors [J]. *Phys. Rev. Lett.*, 2003, **90**(21): 216601-4.

[2] Stevens M J, Smirl A L, Bhat R D R, *et al*. Quantum interference control of ballistic pure spin currents in semiconductors [J]. *Phys. Rev. Lett.*, 2003, **90**(13): 136603-6.

[3] Johnson M, Silsbee R H, Interfacial charge-spin coupling: Injection and detection of spin magnetization in metals [J]. *Phys. Rev. Lett.*, 1985, **55**(17): 1790-3.

[4] Fiederling R, Kein M, Reuscher G, *et al*. Injection and detection of a spin-polarized current in a light-emitting diode [J]. *Nature*, 1999, **402**(7): 787-790.

[5] Wang B G, Wang J, Guo H. Quantum spin field effect transistor [J]. *Phys. Rev. B*, 2003, **67**(09): 092408-11.

[6] Li C, Yu Y, Wei Y, *et al*. Nonadiabatic quantum spin pump: Interplay between spatial interference and photon-assisted tunneling in two-dimensional Rashba systems [J]. *Phys. Rev. B*, 2007, **75**(3): 035312-9.

[7] Busl M, Platero G. Spin-polarized currents in double and triple quantum dots driven by ac magnetic fields [J]. *Phys. Rev. B*, 2010, **82**(20): 205304-10.

[8] Datta S, Das B. Electronic analog of the electro-optic modulator [J]. *Appl. Phys. Lett.*, 1990, **56**(7): 665-7.

[9] Nitta J, Akazaki T, Takayanagi H, *et al*. Gate control of spin-orbit literaction in an inverted In0.53Ga0.47As/In0.52Al0.48As heterostructure [J]. *Phys. Rev. Lett.*, 1997, **78**(7): 1335-8.

[10] Souma S, Nikolic B K. Modulating unpolarized current in quantum spintronics: Visi-bility of spin-interference effects in multichannel Aharonov-Casher mesoscopic rings [J]. *Phys. Rev. B*, 2004, **70**(19): 195346-56.

[11] Chen K W, Chang C R. Quantum interference and spin polarization on Rashba double quantum dots embedded in a ring [J]. *Phys. Rev. B*, 2008, **78**(23): 235319-25.

[12] Chi F, Zheng J. Spin-polarized current and spin accumulation in a three-terminal two quantum dots ring [J]. *Appl. Phys. Lett.*, 2008, **92**(17): 062106-8.

[13] Sun Q F, Xie X C. Spontaneous spin-polarized current in a nonuniform Rashba interaction system [J]. *Phys. Rev. B*, 2005, **71**(15): 155321-6.

[14] Sun Q F, Wang Jian, Guo Hong. Quantum transport theory for nanostructures with Rashba spin-orbital interaction [J]. *Phys. Rev. B*, 2005, **71**(16): 165310-1.

[15] Jauho A P, Wingreen N S, Meir Y. Time-dependent transport in interacting and non-interacting resonant-tunneling systems [J]. *Phys. Rev. B*, 1994, **50**(8): 5528-44.

[16] Matsuyama T, Kursten R, Merkt U. Rashba spin splitting in inversion layers on p-type bulk InAs [J]. *Phys. Rev. B*, 2000, **61**(23): 15588-91.